Available online at www.sciencedirect.com
ScienceDirect
Energy 32 (2007) 1855–1870
ENERGY
www.elsevier.com/locate/energy

An empirical validation of the daylighting algorithms and associated interactions in building energy simulation programs using various shading devices and windows

Peter G. Loutzenhiser[a,*], Gregory M. Maxwell[b], Heinrich Manz[a]

[a]Swiss Federal Laboratories for Materials Testing and Research (EMPA), Laboratory for Building Technologies, Ueberlandstrasse 129, CH-8600 Duebendorf, Switzerland
[b]Department of Mechanical Engineering, Iowa State University, Ames, Iowa 50011, USA

Received 8 September 2006

Abstract

Empirical validation of building energy simulation programs is an important technique in examining the effectiveness and accuracies of implemented algorithms. In recent years, daylighting algorithms incorporated in building energy simulation programs have become increasingly sophisticated in their abilities to predict the illuminance, light power reductions, and the associated thermal load interactions. The focus of this study was to examine measured and simulated light levels in an actual building constructed for research purposes. Daylighting models were constructed in EnergyPlus and DOE-2.1E and the predicted illuminance and light power were compared with measurements; an assessment of heating and cooling interactions using a variable-air-volume reheat (VAVRH) system was also performed by analyzing reheat coil powers for the VAV boxes. The average differences from EnergyPlus for reference point daylight illuminance, light power, and reheat coil power predictions were within 119.2%, 16.9%, and 17.3%, respectively. DOE-2.1E predicted reference point daylight illuminances were within 114.1%, light powers were within 26.3%, and reheat coil power were within 25.4%.

Keywords: Daylighting; Empirical validation; Building energy simulation tools

1. Introduction

During the last 30 years, engineers and architects have increasingly relied on building energy simulation programs to design and retrofit buildings. Increased computer capacity has allowed for the implementation of complex control algorithms used in modern structures to be simulated by various programs. One such control strategy is daylighting control. Daylighting controls take advantage of daylight entering the space through windows, skylights and/or light wells and adjust the amount of artificial light to the space to control the light level at a given point. Typically, a controller mounted in the ceiling measures the illuminance on a reference plane. When the illuminance on this reference plane deviates from a specified set point, the controller sends feedback to dimmable ballasts which cause the lights to dim or illuminate to maintain prescribed light levels. Building energy simulation programs combine room geometry and surface optical properties, window information, and window shading (if installed) into the algorithms to compute illuminance(s) at a reference point(s) in the zones. This information, along with detailed lighting and ballast specifications, is used to calculate the amount of light dimming required to maintain a fixed illuminance.

Important and necessary components for evaluating these types of programs are rigorous validations. Judkoff [1] identifies three types of validations for building energy simulation programs: analytical validations, program-to-program comparisons, and empirical validations. In analytical validations, the building energy simulation programs are configured according to a case where the

*Corresponding author. Tel.: +41 44 823 43 78; fax: +41 44 823 40 09.
E-mail address: peter.loutzenhiser@empa.ch (P.G. Loutzenhiser).

0360-5442/$ - see front matter © 2007 Elsevier Ltd. All rights reserved.
doi:10.1016/j.energy.2007.02.005

Nomenclature

D_i	difference between experiment and predicted values for a given value
$\overline{D}$	mean difference for a given array
$\lvert\overline{D}\rvert$	mean absolute difference for a given array
D_{max}	maximum difference between experimental and predicted values for a given array
D_{min}	minimum difference between experimental and predicted values for a given array
D_{rms}	root mean squared difference between experimental and predicted values for a given array
$D_{95\%}$	95th percentile of the differences between experimental and predicted values for a given array
N	number of points in the array that were used for the analysis
$OU_{Experiment}$	95% credible limits or overall uncertainty from experiment
$OU_{EnergyPlus}$	95% credible limits or overall uncertainty from MCA
$\overline{OU}$	average overall uncertainty calculated for 95% credible limits
UR_i	uncertainty ratio for a given hour, no units
$\overline{UR}$	average uncertainty ratio for a given array, no unit
UR_{max}	maximum uncertainty ratio for a given array, no units
UR_{min}	minimum uncertainty ratio for a given array, no units
$\bar{x}$	arithmetic mean for a given array
x_{min}	minimum quantity for a given array
x_{max}	maximum quantity for a given array

analytical solution is known. Program outputs are then compared with the analytical solution. The advantages for this type of validation include: no input uncertainties, an absolute truth standard, and low costs; the primary disadvantage is that analytical solutions are limited to very simple cases. In program-to-program comparisons, the same input specifications are used and the outputs from each program are then compared. The advantages include: relatively inexpensive and straightforward and the validations can be as complex as necessary. The disadvantage is that there is no truth standard; so it is impossible to ascertain which program (s), if any, is (are) correct. For empirical validations, an actual experiment is run and then modeled in building energy simulation programs. The advantages are that there is an absolute truth standard within experimental uncertainty limits, and it can be as complex as required. The primary disadvantage is that empirical validations are expensive to perform.

Numerous daylighting algorithms have been developed and validated that explore different types of shading devices and illuminance predictions [2–6]. The International Energy Agency's Task 21 [7] was assembled to investigating daylighting for design tools and software in buildings. One of the most popular daylighting algorithms used in the design of buildings [8] was installed in DOE-2.1E and is analyzed in this paper.

Different facets of the DOE-2.1E daylighting algorithm has been already explored in earlier studies, including numerous empirical validations [9–13] and several studies that use the program as a tool for optimizing the daylighting performance of buildings [14–17]. Other empirical validations that did not emphasize daylighting have been performed in the PASSYS project [18–20], IEA Annex 21/Task 8 [21], and IEA Task 34/Annex 43 [22–25] that explore different facets of the building envelope and the associated solar gains with and without solar shading devices.

The focus of this research is to evaluate the daylighting algorithms and connected load interactions in EnergyPlus [26] and DOE-2.1E [27]. The experiment was performed in test rooms in a research facility in conjunction with the International Energy Agency's Task 34/Annex 43 Subtask C. For this study, various shading devices (internal and external) and windows were installed in different combinations to assess the performances of each building energy simulation program. Various statistical parameters were employed to compare the results. Experimental uncertainties were computed and a Monte Carlo analysis (MCA) was used to quantify how uncertainties in program input parameters (thermophysical properties and instrumentation uncertainties) propagated through a building energy simulation program (in this case EnergyPlus) and impacted output predictions.

2. Facility layout

The building where the research was performed is uniquely equipped for empirical validations and meets all nine criteria for a high quality validation data set [19]. The facility is located on the campus of a community college in Ankeny, Iowa USA. The structure is comprised of eight test rooms, a computer room, offices, two classrooms and other rooms necessary for the support and operation of the facility. A drawing of the building is shown in Fig. 1. The test rooms were constructed in symmetrical pairs to provide side-by-side testing with exposures to nearly identical outside thermal loads. The volume and floor area of the test rooms are 61.23 m^3 and 23.63 m^2, respectively. Three pairs of test rooms are located at the perimeter of the building (east, south, and west) and the other two test rooms are situated inside the facility. There are three air-handling units (AHUs) in the facility. Test rooms denoted as A and B are served by different two nearly identical AHUs; the other AHU serves the rest of the facility. The

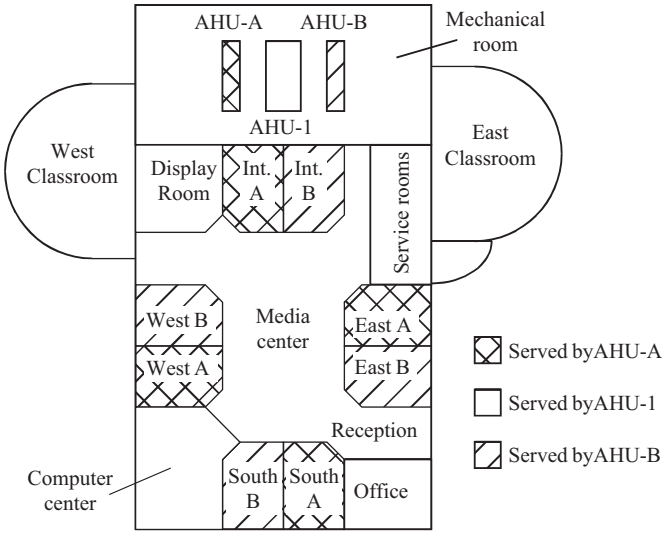

Fig. 1. Facility layout (courtesy of [28]).

Fig. 2. Photograph of the South B test room during a daylighting test.

building also contains a weather station, pyranometer, pyrheliometer, precision infrared radiometer, and numerous exterior light sensors. Additional information concerning the construction and layout of the building is provided by [28].

3. Experiment

A daylighting experiment was run from July 1 to July 7, 2005 using variable-air-volume systems with electric reheat coils (VAVRH) to evaluate the performances of building energy simulation programs. For the experiment, the supply air temperatures from the AHUs were fixed at 13 °C and the temperature rise from the AHU to the inlets of the VAV terminal units associated with heat duct gain was ~0.6 K during the experiment. The maximum and minimum room airflow rates for the exterior test rooms were 1000 and 800 m^3/h, respectively. The path of the return air was through the plenum spaces. The room heating and cooling temperature set points for all the test rooms were 22 and 23 °C, respectively. One stage of installed baseboard heat with rated power of ~890 W operated during the entire experiment to add a sensible cooling load. In the exterior test rooms, box fans, used to reduce temperature stratification, were mounted near the ceiling during the experiment with a measured power of ~125 W. Specific information concerning other aspects of the experiment pertaining to the daylighting setup is contained in this section. Fig. 2 contains a photograph of a test room taken during a daylighting experiment.

3.1. Windows, shading devices, and interior surfaces

Various windows and shading devices were installed in the exterior test rooms. Brief descriptions of specifications of the shading devices and windows installed for this experiment are presented in this section. Shading screens, mini-blinds (motorized and fixed), and exterior fins were configured in different combinations with windows shown in Table 1. A description of the properties and installation of the windows, interior shading devices, and exterior fins is provided below.

3.1.1. Windows

Three different types of windows were installed for each pair of test rooms. Optical properties and the thermal transmittances of the windows are provided in Table 2. (Note: These windows were already installed before this work was started; the relatively low thermal quality of these types of glazing was considered unimportant for daylighting studies.)

3.1.2. Interior shading devices

Interior mini-blinds with white slats and white shading screens were installed in four of six exterior test rooms (Table 1). Optical properties of the blind slats and the shading screens were measured. The integral transmittance and reflectance of the shading screen and the reflectance of the blind slats were computed according to EN 410 [29] using Glad software [30] using wavelength dependent near direct-hemispherical measurements taken from 250 to 2500 nm. The hemispherical emittance of the blind slats was also measured; a summary of these properties is shown in Table 3.

In the East A test room, motorized mini-blinds were installed. The blinds were designed to block beam radiation from entering the room. Solar angles were calculated according to [31] using the building location and orientation to derive a control algorithm used to vary the blade angles so that the slats were always normal to the sun during the morning when beam irradiance entered the space. In the afternoon, the blinds slats were controlled to the horizontal position and then closed at 16:00 Central Standard Time (GMT-6). When in the horizontal position,

Table 1
Test rooms shading and window configurations for the experiment

Test room	Window type	Interior window treatment	Exterior window treatment
East A	25.2 mm low-E#3 glazing system	Motorized mini-blinds	None
East B	25.2 mm low-E#3 glazing system	Fixed slat angle horizontal mini-blinds	None
South A	25.2 mm clear glass glazing system	Nysan roller shades	None
South B	25.2 mm clear glass glazing system	Fixed slat angle horizontal mini-blinds	None
West A	25.2 mm low-E#2 glazing system	Nysan roller shades	Exterior fins
West B	25.2 mm low-E#2 glazing system	None	Exterior fins

Table 2
Test room window properties

Type	25.2 mm OA Low-E #3	25.2 mm OA Low-E #2	25.2 mm OA clear glazing
Layers	6 mm Clear (103)[a] 13.2 mm airspace 6 mm Lof Pyro Low-E #3 (9924)[a]	6 mm VE3-55 #2 (6059)[a] 13.2 mm airspace 6 mm Clear (103)[a]	6 mm Clear (103)[a] 13.2 mm airspace 6 mm Clear (103)[a]
Visible tansmittance	73%	23%	79%
Solar transmittance	52%	14%	61%
Visible light-exterior reflectance	17%	6%	14%
Visible light-interior reflectance	16%	15%	14%
Solar exterior reflectance	15%	10%	11%
ASHRAE U-value winter Nighttime	1.87 W/m^2-K	1.76 W/m^2–K	2.68 W/m^2-K
ASHRAE U-value summer Daytime	2.0 W/m^2-K	1.87 W/m^2–K	2.81 W/m^2-K
Shading coefficient	0.79	0.26	0.81
Solar heat gain coefficient	0.66	0.22	0.70
Relative heat gain	497.7 W/m^2	176.4 W/m^2	533 W/m^2

Note: All properties are center–pane values.
[a]ID number from the Window 5.2a glazing system library.

Table 3
Optical properties of the interior shading devices

Type	Nysan superweave 1000 (10% open) white fabric	White mini-blind slats
Normal visible transmittance, %	30.5	0.0
Normal solar transmittance, %	30.4	0.0
Normal visible reflectance, %	67.3	73.1
Normal solar reflectance, %	59.4	63.9
Hemispherical emittance, %	—	72.1

the inner edges of the blind slats were 38.1 mm from the inner glass pane of the window. In the East B and South B test rooms, mini-blinds were installed with the slats fixed in the horizontal position 76.2 mm from the inner edges of the blind slats to the inner pane of glass. Nysan Superweave 1000 (10% openness factor) shading screens were installed in the West A and South A test rooms. The shading screens were mounted 108.0 mm from the inner glass pane.

3.1.3. Exterior fins

Opaque exterior fins were constructed around the windows of the west test rooms. A dimensioned drawing of the fins is shown in Fig. 3. The exterior fins were constructed out of a dark brown polymeric material to minimize reflection from the fins through the windows to the space.

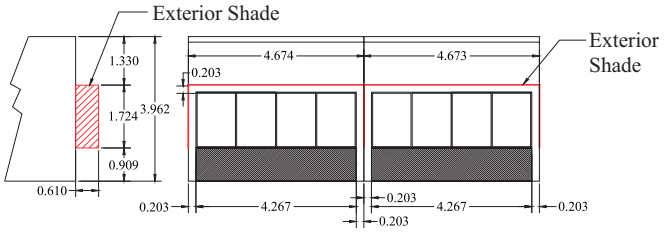

Fig. 3. Drawing and dimensions in meters of the exterior fins for west test rooms.

3.1.4. Interior surfaces

Samples taken from the interior surfaces of the test rooms were measured from 250 to 2500 nm; visible and solar properties of these surfaces were computed according to EN 410 [29] using Glad Software [30] and are provided in Table 4.

3.2. Lighting and daylighting controls

Four fluorescent light fixtures with dimmable ballasts were mounted in each exterior test room. A light sensor with a 180° field of view, located on a table near the center of each room shown in Fig. 4, provided feedback to the

Table 4
Optical properties for the interior surfaces

Surface	Solar reflectance, %	Visible reflectance, %
Ceiling	49.8	55.7
Walls	78.8	83.6
Floor	26.4	10.3

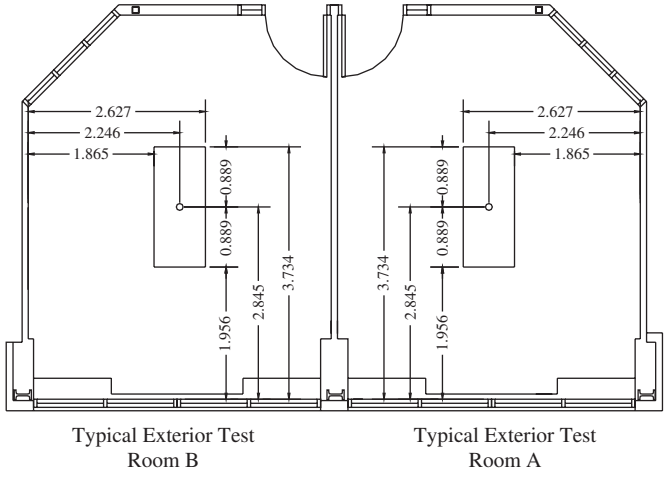

Fig. 4. Light sensor reference point (the sensor height is 0.724 m from the floor).

lighting control algorithm which maintained the illuminance at the reference point by controlling the ballasts. The lights were turned off when they were at maximum dimming and illuminance exceeded set point, the lights were then turned back on when the illuminance dropped 108 Lux below the set point. Table 5 contains a list of maximum and minimum light power (including ballasts) measured prior to the experiment and illuminance set points and at minimum lighting and corresponding reference point illuminance for the exterior test rooms. Measurements prior to the experiment indicated a linear relationship between reference point illuminance and light power in the absence of daylight in the space (the measurements were taken at night) and are shown for all exterior test rooms in Fig. 5.

4. Simulations

This section contains brief narratives concerning the modeling of the facility in EnergyPlus and DOE-2.1E. Detailed architectural drawing of the facility, construction material properties, and optical properties were used to model the facility along with the information described in Section 3. Weather parameters which included: dry-bulb temperature, relative humidity, barometric pressure, direct-normal solar irradiance, global horizontal solar irradiance, global horizontal infrared irradiance, global horizontal illuminance, and global vertical illuminance on the east, west and south exterior façade were measured in one minute increments. During the experiment, spaces adjacent to the test rooms were maintained at nearly the same air temperature as the test rooms to provide near-adiabatic conditions. For verification, the adjacent space air temperatures were also measured and could be used as input into the building energy simulation programs. The ground temperatures used in both building energy simulation programs were calculated using the EnergyPlus ground temperature preprocessor program using a TMY2 weather file for Des Moines, Iowa USA; the ground temperature for a perimeter rooms in July was computed as 19.6 °C.

4.1. Energy plus

A simulation model of the facility was constructed in EnergyPlus. The construction elements adjacent to occupied zones in the building were modeled as adiabatic boundaries. The internal heat loads in the test rooms were considered purely sensible 97% convective loads and the light fixtures were modeled as recessed fluorescent lamps. Weather data measured at the facility were averaged in 10 min intervals and used as boundary conditions. Because diffuse global solar irradiance was not measured at the facility but is a required input, it was computed using the solar altitude angles calculated from EnergyPlus (to ensure the same solar angle algorithm was used) and direct-normal and global horizontal solar irradiances measured with the solar instruments.

The "DAYLIGHTING:DETAILED" model in EnergyPlus was used because of its configuration closely matched the provided inputs compared with the other two available models in EnergyPlus. The inputs required for this model included: maximum and minimum light powers and corresponding illuminances (input as ratios), a daylight reference point(s) (a maximum of two), and illuminance set points. This model is similar to the daylighting model used in DOE-2.1E with two additional sky luminance distributions [32]. The vertical solar irradiances and illuminances on the exterior façades were computed in the program using a Perez 1990 [33] model and solar irradiance inputs. The ground reflectance estimated using measurements from [23,34] was approximated as 15%.

The windows were modeled in Window 5.2a [35] and an output file was used that accounted for angular dependent properties. The window spacer and frame were modeled as a generic aluminum spacers and aluminum frames, respectively. The shading screens were modeled as diffuse transmitters. The shading screens were described in the program using normal visible and solar transmittances and reflectance described in Table 3 and accounted for re-reflections into the space from the window screen using a ray tracing method that assumed infinitely flat plates. EnergyPlus contains a blind model used to estimate the visible and solar transmittance of the blind assemblies. This model assumes that the blinds are perfectly flat diffuse reflectors which are infinitely long. Cross-strings for two-dimensional configuration factor calculations were used for blind slats and the window described by [32]. The heat

Table 5
Maximum and minimum light power and corresponding illuminance

Test room	Maximum light power, W	Minimum light power, W	Setpoint illuminance, Lux	Illuminance without daylighting at reference point for minimum light power, Lux
East A	356	86.1	645	17.5
East B	362	89.3	645	29.2
South A	364	88.1	700	34.1
South B	362	89.3	700	26.9
West A	362	88.4	645	28.7
West B	348	86.9	645	23.6

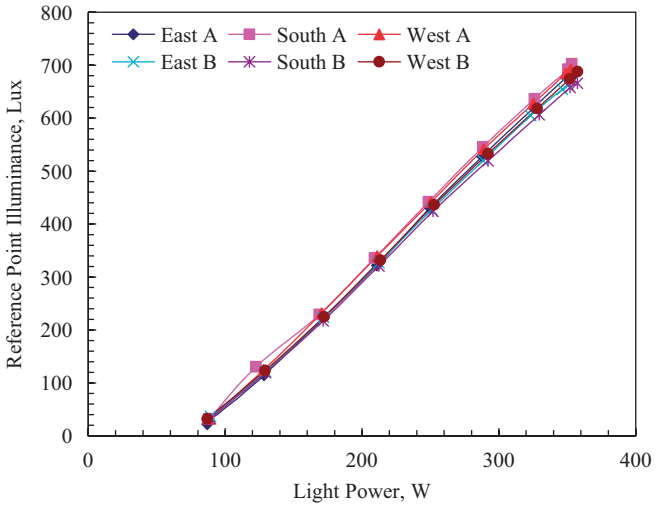

Fig. 5. Measured light power versus reference point illuminance for the test rooms.

transfer between the window and the shading devices was calculated using ISO 15099 [36] assuming natural buoyancy; this was performed as an iterative procedure in the program. The exterior fins were modeled as opaque non-reflecting fins around the west windows. The HVAC equipment was auto-sized in the program and zone heating and cooling set points for temperatures and maximum and minimum airflow rates were fixed in the model.

A detailed algorithm as a function of surface orientation and surface temperatures was used to quantify convective heat transfer and approximate geometric view factors in the program were employed to calculate the radiative heat exchange between surfaces.

4.2. DOE-2.1E

The facility was also modeled in DOE-2.1E. The test rooms were modeled as cuboids with room widths and heights that corresponded with the actual dimensions of the space and an equivalent room length corresponding to the room volume was implemented. Custom weighting factors were used in the program to account for transient heat transfer of the building elements. The test rooms' internal loads were considered sensible and 97% convective and recessed light fixture models were employed. The interior walls adjacent to occupied areas were modeled as adiabatic boundaries. The daylighting model in DOE-2.1E is described in detail by [8]. Hourly averaged weather data measured at the facility were put into TMY2 weather format and used as inputs into the program. Measured global horizontal and direct-normal solar irradiances were used to calculate the global vertical irradiances and illuminances on the east, south, and west façades using the Perez 1990 model and the same ground reflectance as in EnergyPlus. In TMY2 weather, it is impossible to input global horizontal infrared irradiance; therefore the opaque sky cover was calculated by reversing the code algorithm for calculating infrared global horizontal irradiance used in the TMY2 weather file [37,38].

The windows were modeled in Window 5.2a, which accounted for angular dependent properties. Generic aluminum spacers and frames were used. Integral solar and visible shading transmittances were employed for simulating the shading screens. DOE-2.1E did not account for reflected light back into the space from the shading screens. Because surface temperatures of the inner glass panes and the shading screen, and the air temperatures in the gap were not known, the heat transfer in the air gap between the inner glazing and shading screen was estimated using EN ISO 6946 [39] for an unventilated air layer. The exterior fins over the east windows were described in the input file as opaque non-reflecting surfaces. Currently, DOE-2.1E does not have an algorithm to model mini-blinds and there are no subsidiary software designed to be used in conjunction with this building energy simulation program; therefore, comparisons for the test rooms with mini-blinds did not include results from DOE-2.1E.

Combined design heat transfer coefficients that accounted for construction element orientations were taken from [31] for all construction elements (floor, ceiling, and walls) to estimated total impact of convective and radiative heat transfer for the interior surfaces. This was done because construction element surface temperatures in the program were not known.

5. Uncertainties

Accounting for experimental uncertainties is of utmost importance when performing empirical validations. For this study, the experimental uncertainties of measured

parameters that were calculated and compared with program outputs. The uncertainties of program outputs as a function of program inputs were accounted for by using MCA. Ninety-five credible limits from these calculations were used in the statistical analysis to assess the overall performance of the building energy simulation programs.

5.1. Experimental uncertainties

The uncertainties of experimental measurements were estimated based on manufacturers' specifications assembled by [28]. Using a criterion proposed by [40], the uncertainties were considered Bayesian and estimated according to a uniform probability distribution function (pdf); ninety-five percent credible limits were then calculated. Specific information about instruments used for measuring parameters for comparisons and the uncertainties is given in Table 6.

5.2. Monte Carlo analysis

An MCA was used to evaluate how uncertainties of input parameters propagated through the building energy simulation programs and impacted simulation outputs and was performed using EnergyPlus. A thorough description of how this analysis was performed is provided by [23]. Input uncertainties for measuring equipment were again taken from information provided by product manufacturers that were compiled by [28]. Thermophysical and optical property uncertainties were estimated to be $\pm 5\%$ and $\pm 1\%$ of the quantity, respectively. The physical dimensions of the rooms were not perturbed because of associated interactions with other test room. Because the uncertainties were of Bayesian nature, they were perturbed in the MCA according to a uniform pdf. For this study, 120 runs were used to estimate 95% credible limits assumed normal by the Central Limit Theorem and verified using a Lilliefors Test for a Normal Distribution at a 1% significance level. Because it was impossible to modify the Window 5.2a output file, visible and solar integral transmittances and reflectance for each pane were entered into the program and perturbed for the MCA.

Table 6
Data parameters and equipment

Measured parameter	Manufacturer	Model number	Accuracy, %
Illuminance	LI-COR	LI-190SZ	± 5
Light power	Ohio semitronics	GH-002C	± 0.2
Reheat power	Ohio semitronics	GH-020-CY38	± 0.2

6. Results

Several zone output parameters from the building energy simulation programs were compared with hourly averaged quantities measured at the facility during the experiment for the exterior test rooms. These outputs included: illuminance at the reference point due to daylight, light power, and reheat coil power. Because the minimum airflow rate set points in the test rooms were relatively high, reheat was required during most of the test to overcome the ventilation load of the entering air; therefore, the airflow rates generally remained at the minimum position and were not compared.

Fig. 6 contains measured direct-normal and global horizontal solar irradiances. The global exterior illuminances on the test room façades (east, south, and west) and on the horizontal plane were measured during the experiment but were not an output from either program. From this information, hypotheses can be made to assess general trends expected with respect to daylight in the test rooms. The exterior global illuminances are plotted in Fig. 7.

From these plots, it can be seen that there were initially two sunny days, followed by two relatively cloudy days, and, finally, again three moderately sunny days. The global vertical illuminances provide information concerning the amount of potential visible light incident upon the windows (this is reduced for the west test rooms where exterior fins were installed). Because of the high path that the sun takes across the sky during a day in July, beam illuminances and solar irradiances were never

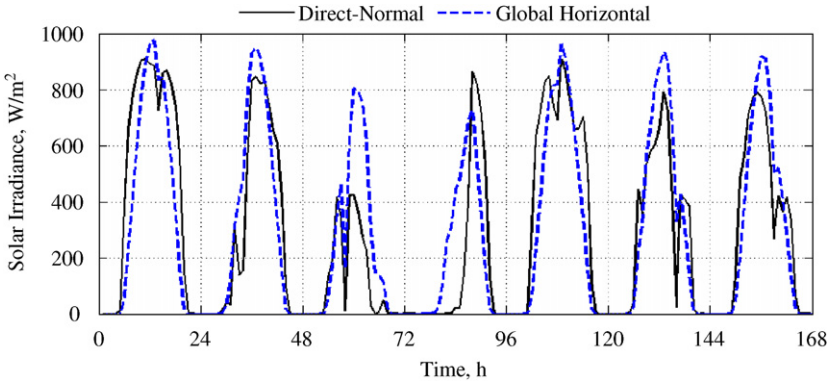

Fig. 6. Direct-normal and global horizontal solar irradiance measurements during the experiment.

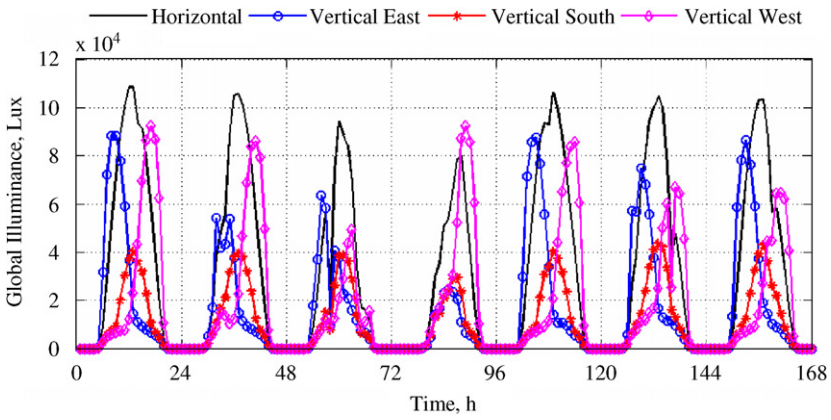

Fig. 7. Horizontal and vertical global exterior illuminance.

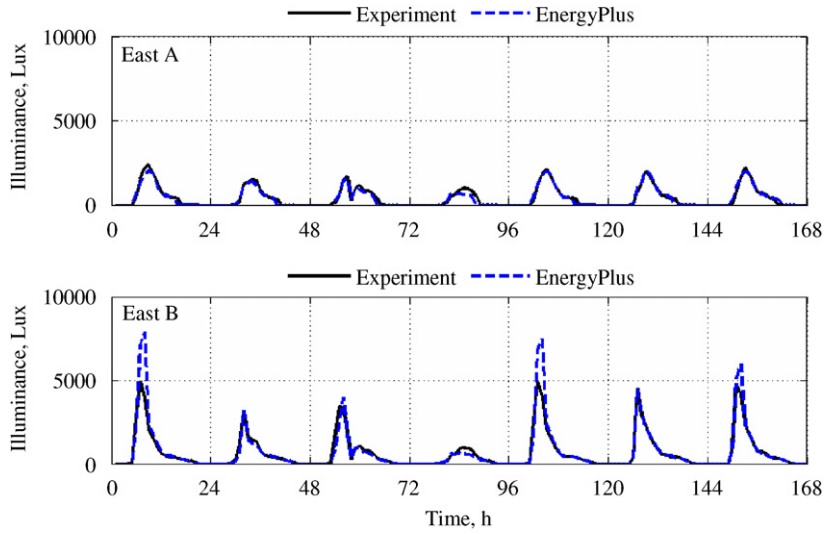

Fig. 8. Reference point daylight illuminance for the east test rooms.

incident upon the south windows but were incident in the morning and evenings on the east and west windows, respectively.

The statistical analysis proposed by [22] was used to assess the performances of the building energy simulation programs. An important parameter is the uncertainty ratio shown in Eq. (1). If this parameter is less than or equal to unity, then the programs were considered validated within 95% credible limits.

$$UR_i = \frac{|D_i|}{OU_{i,Experiment} + OU_{i,EnergyPlus}}. \quad (1)$$

In order not to divide by zero when computing the uncertainty ratios, data were only analyzed if the sum of the uncertainties (experimental and MCA) for the daylight reference point illuminance, light power, and reheat power exceeded 1.0 Lux, 1.0 W, and 1.0 W, respectively, which were arbitrarily chosen for mathematical reasons to ensure that the uncertainty ratio never exceeded the absolute differences. The numbers of values used for the analyses of an array are also given in the statistical comparisons.

6.1. Daylight illuminance

The daylight illuminances were predicted at the reference points in the exterior test rooms. The experimental daylight illuminances were calculated by subtracting from the measured illuminance the illuminances from the artificial lights using light power versus total illuminance relationships from Table 5. The results from the east, south and west test rooms are presented in this section.

In the east test rooms, interior mini-blinds were installed over the LOW-E #3 windows. During the morning, the test rooms were subjected to beam solar irradiation incident on the outer window surface. The blinds slats were automatically adjusted in the A Test Room to ensure that only diffuse solar irradiation entered the rooms, while in the B Test Room, blind slats in the horizontal position did little to impede beam radiation during sunrise. From Table 2, a maximum of 73% of the visible light penetrated the space at normal incident angles through the windows when the mini-blinds failed to stop beam radiation. The measured and predicted daylight illuminances for the east test rooms are shown in Fig. 8.

The south test rooms had double clear glazing windows. Shading screens and mini-blinds in the horizontal positions were installed in the A and B Test Rooms, respectively. During this time of the year, the sun takes a high path across the sky and so beam radiation was never incident upon the outer window pane of south-facing windows. Therefore, only diffuse light enters the space. Daylight illuminance measurements and predictions at the references points are shown in Fig. 9.

In the west test rooms, exterior fins were installed over LOW-E #2 windows to reduce the beam radiation entering the space. Beam radiation was only incident on the outer window panes in the evening when the sun was setting. Predictions are compared with measurements in Fig. 10 for reference point daylight illuminance.

An assessment of the overall performance of the programs for each test room was performed by employing statistical parameters for each test room. Table 7 contains the comparisons for the daylight reference point illuminance for the exterior test rooms and corresponding predictions from the building energy simulation programs.

6.2. Light power

Dimmable ballasts were used to maintain reference point illuminance on the table light sensor (used as a reference point in the programs). The measured and predicted light powers for the east, south, and west test rooms and statistical comparisons are provided in this section. Fig. 11

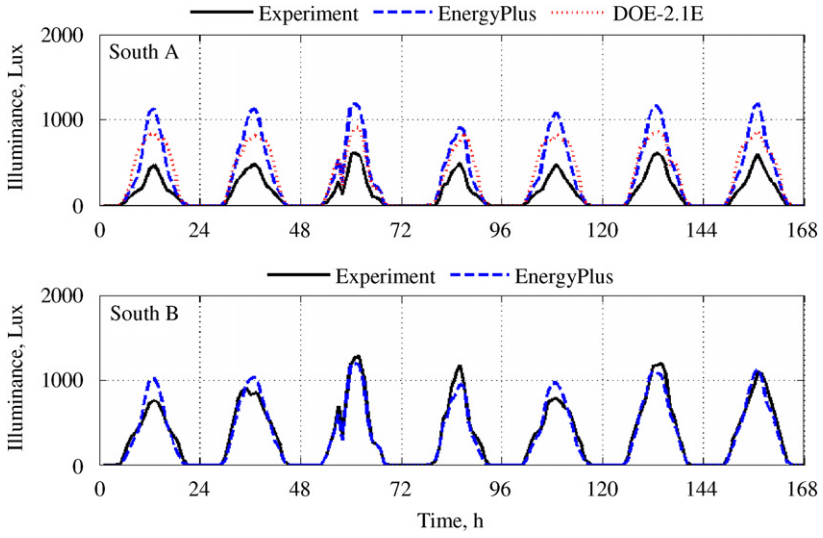

Fig. 9. Reference point daylight illuminance for the south test rooms.

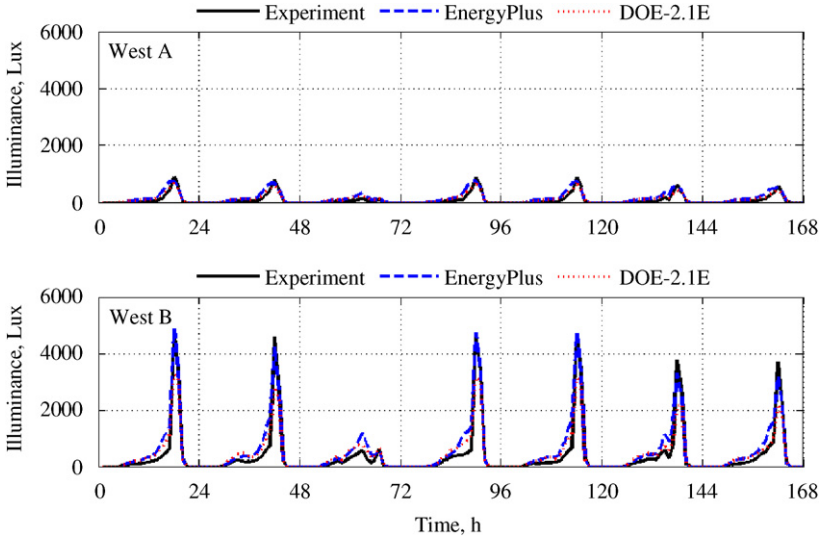

Fig. 10. Reference point daylight illuminance for the west test rooms.

Table 7
Statistical analysis for the room daylight illuminance at the reference point

	Units	East A		East B		South A			South B		West A			West B		
		Exp.	EnergyPlus	Exp.	EnergyPlus	Exp.	EnergyPlus	DOE-2.1E	Exp.	EnergyPlus	Exp.	EnergyPlus	DOE-2.1E	Exp.	EnergyPlus	DOE-2.1E
$\bar{x}$	Lux	692.8	648.6	1050.3	1132.8	248.1	543.7	531.1	545.5	524.8	132.0	220.8	172.5	653.7	862.6	692.9
s	Lux	640.4	608.7	1214.5	1653.9	167.9	365.8	264.5	334.1	355.5	210.8	214.4	161.1	1140.1	1106.9	791.9
x_{max}	Lux	2375.0	2014.2	4937.0	7859.4	609.0	1191.0	905.6	1272.0	1186.5	873.0	744.8	666.9	4593.0	4880.4	3238.7
x_{min}	Lux	0.0	2.1	12.0	10.3	0.0	39.6	32.7	28.0	9.3	0.0	10.5	11.6	0.0	32.1	30.9
$\overline{D}$	Lux	—	44.1	—	−82.5	—	−295.6	−283.0	—	20.8	—	−88.8	−40.5	—	−208.9	−39.2
$\lvert\overline{D}\rvert$	Lux	—	109.2	—	259.0	—	295.6	283.0	—	80.3	—	100.9	70.2	—	246.0	265.4
D_{max}	Lux	—	550.6	—	3940.4	—	677.9	552.8	—	277.0	—	305.9	224.9	—	939.5	1763.6
D_{min}	Lux	—	0.6	—	0.5	—	19.9	20.2	—	0.3	—	0.2	3.3	—	6.5	9.8
D_{rms}	Lux	—	167.4	—	661.4	—	359.1	317.1	—	101.4	—	127.4	81.3	—	343.8	430.1
$D_{95\%}$	Lux	—	374.4	—	1149.1	—	618.2	503.4	—	205.8	—	278.6	130.8	—	754.8	1354.3
$\overline{OU}$	Lux	39.2	11.2	59.4	18.4	14.0	16.5	—	30.9	19.2	7.5	21.9	—	37.0	62.7	—
$\overline{UR}$		—	4.3	—	3.1	—	9.9	12.0	—	2.5	—	5.9	5.2	—	4.2	4.2
UR_{max}		—	60.7	—	20.5	—	32.1	26.8	—	13.1	—	10.4	12.7	—	13.7	12.8
UR_{min}		—	0.0	—	0.0	—	4.5	3.5	—	0.0	—	0.0	0.1	—	0.0	0.1
$\lvert\overline{D}\rvert\bar{x}\times 100\%$	%	—	15.8	—	24.7	—	119.2	114.1	—	14.7	—	76.4	53.2	—	37.6	40.6
$\overline{D}/\bar{x}\times 100\%$	%	—	6.4	—	−7.9	—	−119.2	−114.1	—	3.8	—	−67.2	−30.7	—	−32.0	−6.0
N	—	95	95	102	102	96	96	96	102	102	99	99	99	102	102	102

contains plots of the experimental and predicted light power for the east test rooms.

Results for the light power in the south test rooms from the measured and predicted light power are contained in Fig. 12.

Light power measurements and predictions for the west test rooms are shown in Fig. 13. Statistical analyses of the predictions compared with the measurements are presented in Table 8.

6.3. Reheat coil power

The VAVRH system used electric reheat coils to reduce experimental uncertainties. VAV boxes that use electric heat require relatively high minimum airflow rates to satisfy the safety systems which prevent the coils from being energized if the airflow is too low. Heating and cooling temperature set points for the test rooms were used as inputs to the programs with a 1 K temperature dead band. During the experiment, there were only cooling loads in the test rooms because of the internal loads introduced into the space and summertime conditions. However, due to high ventilation rates and the low supply air temperature chosen, the reheat coils in the VAV boxes were nearly always energized.

The measured and predicted reheat powers from the electric coils for the east test rooms are shown in Fig. 14. Reheat power was not required in the east test rooms for only four mornings when beam radiation entered the rooms.

Comparison plots between the measured and predicted reheat powers for the south test rooms are shown in Fig. 15.

Measured and predicted reheat powers for the west test rooms are shown in Fig. 16. Statistical comparisons for the reheat coil power are shown in Table 9.

7. Discussion

The discussion is divided up into three sections: daylight illuminances, light power, and reheat power.

7.1. Daylight illuminance

Strictly speaking with respect to the daylight illuminance predictions, none of the programs predicted daylight illuminance at the reference points within 95% credible limits. The EnergyPlus model performed best in the South B test room and worst in the East B room; in both cases mini-blinds were installed.

General assessments of mini-blind algorithm performances can be seen in the South B and east test rooms. The daylight algorithm performed best when diffuse light entered the space and the mini-blind slats were in the horizontal position. Good agreement was also seen in the East A test room where the blinds were adjusted to prevent beam radiation from entering the space. In the East B test

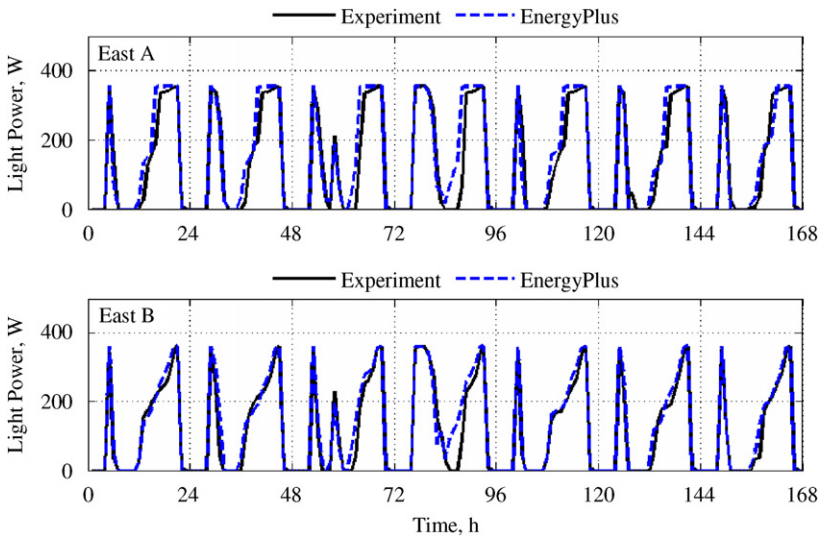

Fig. 11. Light power for the east test rooms.

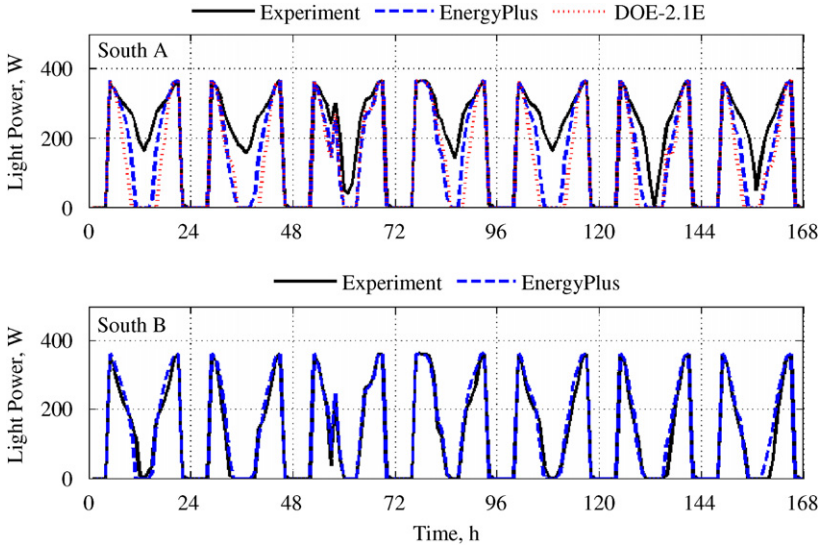

Fig. 12. Light power for the south test rooms.

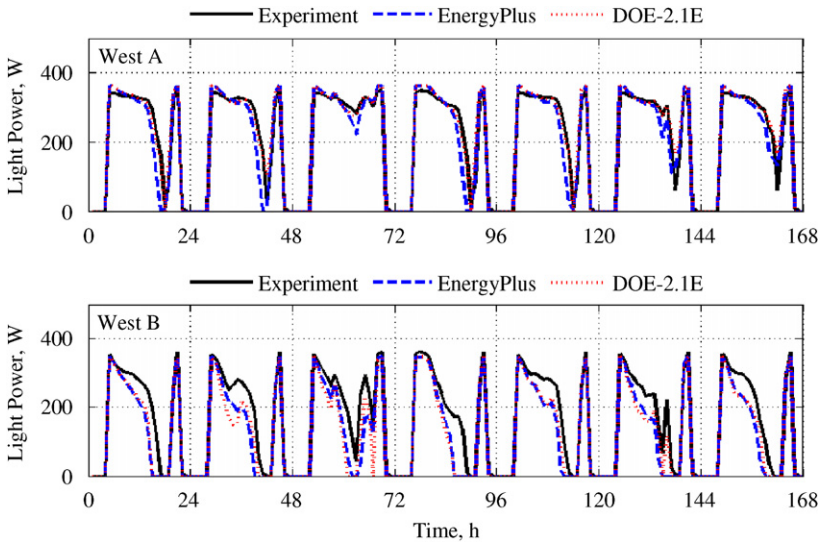

Fig. 13. Light power for the west test rooms.

Table 8
Statistical analysis for the room light power

	Units	East A		East B		South A		South B		West A		West B		
		Exp.	EnergyPlus	Exp.	EnergyPlus	Exp.	EnergyPlus	DOE-2.1E	Exp.	EnergyPlus	Exp.	DOE-2.1E	Exp.	EnergyPlus	DOE-2.1E
$\bar{x}$	W	177.4	195.0	167.8	183.7	302.6	251.4	223.1	229.8	245.2	324.4	325.6	330.9	318.2	304.4	297.3
s	W	153.0	152.6	134.4	133.3	47.7	106.7	127.2	113.8	108.0	29.0	39.4	28.9	43.3	46.4	61.2
x_{max}	W	356.0	356.0	362.0	362.0	364.0	364.0	364.0	362.0	362.0	348.0	362.0	362.0	362.0	348.0	348.0
x_{min}	W	0.0	0.0	0.0	0.0	191.0	0.0	0.0	0.0	16.0	160.0	111.1	212.8	144.0	124.1	0.0
$\overline{D}$	W	—	–17.6	—	–15.9	—	51.2	79.5	—	–15.4	—	–1.1	–6.4	—	13.8	20.9
$\lvert\overline{D}\rvert$	W	—	29.8	—	21.8	—	53.4	81.2	—	21.3	—	14.2	11.2	—	16.4	24.7
D_{max}	W	—	284.8	—	139.3	—	215.8	276.0	—	100.6	—	81.9	52.8	—	52.2	144.0
D_{min}	W	—	0.0	—	0.0	—	0.0	0.0	—	0.0	—	0.3	0.0	—	1.7	4.2
D_{rms}	W	—	57.1	—	35.0	—	79.6	117.9	—	30.0	—	17.7	14.6	—	19.5	34.7
$D_{95\%}$	W	—	132.8	—	90.1	—	171.9	255.0	—	53.4	—	28.3	29.3	—	36.7	66.2
$\overline{OU}$	W	0.4	11.9	0.4	10.9	0.7	11.6	—	0.5	12.8	0.7	11.2	—	0.7	11.0	—
$\overline{UR}$	—	—	3.6	—	2.4	—	3.8	6.2	—	1.6	—	1.5	1.2	—	1.8	3.2
UR_{max}	—	—	36.7	—	15.4	—	33.6	27.1	—	6.4	—	29.1	12.5	—	13.8	31.7
UR_{min}	—	—	0.0	—	0.0	—	0.0	0.0	—	0.0	—	0.0	0.0	—	0.2	0.5
$\lvert\overline{D}\rvert/\bar{x} \times 100\%$	%	—	16.8	—	13.0	—	17.6	26.8	—	9.3	—	4.4	3.5	—	5.2	7.8
$\overline{D}/\bar{x} \times 100\%$	%	—	–9.9	—	–9.5	—	16.9	26.3	—	–6.7	—	–0.3	–2.0	—	4.3	6.6
N	—	119	119	112	112	92	92	92	90	90	91	91	91	48	48	48

room, the model performed well when diffuse radiation entered the space (afternoons and on cloudy days). During the mornings when the sun was incident on the window, the EnergyPlus daylighting/window/shading algorithms significantly over-predicted the magnitude of illuminance at the daylight reference point. These over-predictions could be due to the fact that in its blind model, EnergyPlus assumes the blinds are flat slats, even though the actual blades have curvature. When in the horizontal position and exposed to beam radiation at near-normal incident angles, the flat slat assumption increases the surface area of the window compared with reality; therefore, the flat slat assumptions seems viable for diffuse light in entering the space but over-predicted the illuminance when exposed to beam radiation; however, the results might also be attributed to inadequacies in the beam illuminance transmittance in the blind model.

When shading screens were installed over the windows (South A and West A test rooms), both DOE-2.1E and EnergyPlus were used. While both programs contain similar algorithms for daylight and window (Window 5.2a output files were used) calculations, the EnergyPlus shading model accounted for back reflectances and re-transmission of both visible and solar light between the window and the shading screen, whereas DOE-2.1E used only visible and solar transmittances in its shading calculation and neglected re-transmitted light; therefore, slightly more transmittance in the EnergyPlus model compared with the DOE-2.1E model is expected. Accounting for re-transmitted sunlight resulted in higher daylight illuminance predictions at the reference point in the both South A and West A test rooms compared with DOE-2.1E. Other factors that may have resulted in offsetting errors may also be present.

Both EnergyPlus and DOE-2.1E were used in the west test rooms with exterior fins installed over the windows. During the morning when diffuse light entered the space (Fig. 10), the predictions appear quite accurate. In the afternoon, beam radiation was incident upon exterior fins and when making the transition from the exterior fins to the outer window, both DOE-2.1E and EnergyPlus over-predicted the daylight reference point illuminance for most days. When beam radiation entered the space in the West B test room (where no interior shading was installed), EnergyPlus more accurately predicted reference point illuminances. From these results, the opaque non-reflecting exterior fin model seems plausible.

7.2. Light power

Again, none of the programs were with within the overlapping 95% credible limits from the MCA and experiment (the uncertainty ratios). The MCA credible limits are much higher than the experimental credible limits, primarily due to uncertainties in shading and window optical properties and daylight reference point illuminance set points. One of the limitations was that the

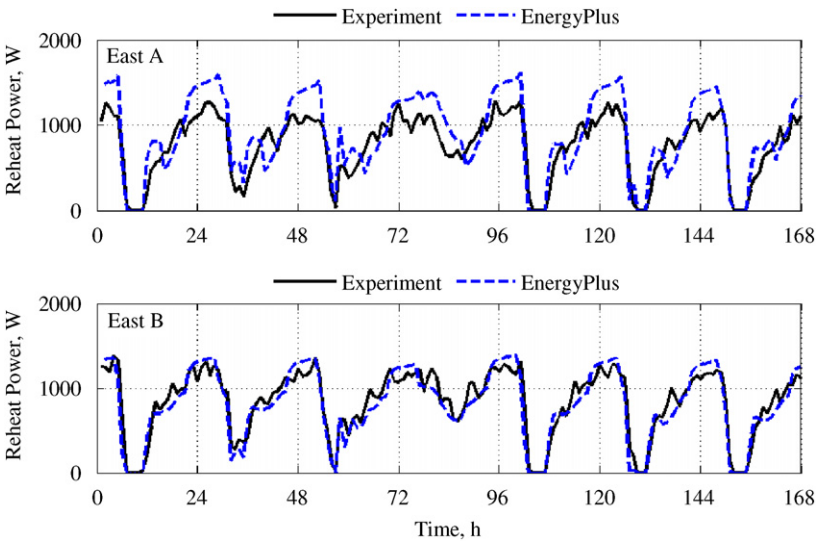

Fig. 14. Reheat coil power for the east test rooms.

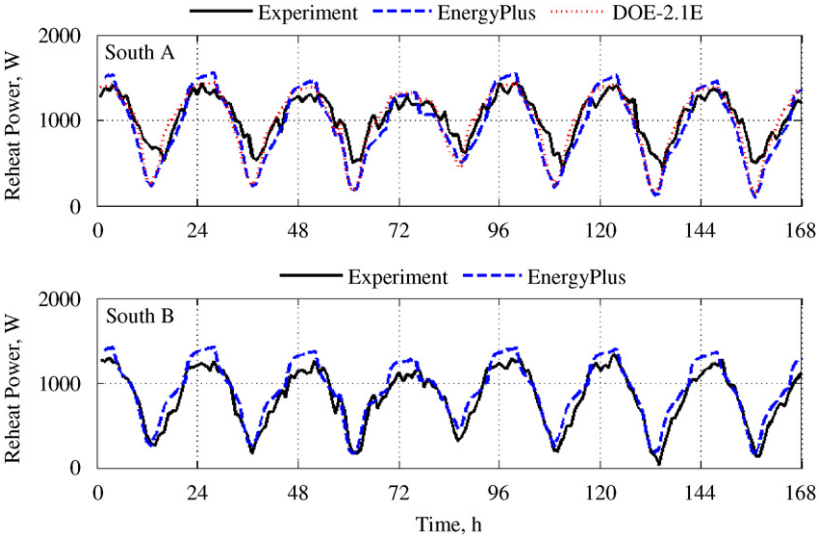

Fig. 15. Reheat coil power for the south test rooms.

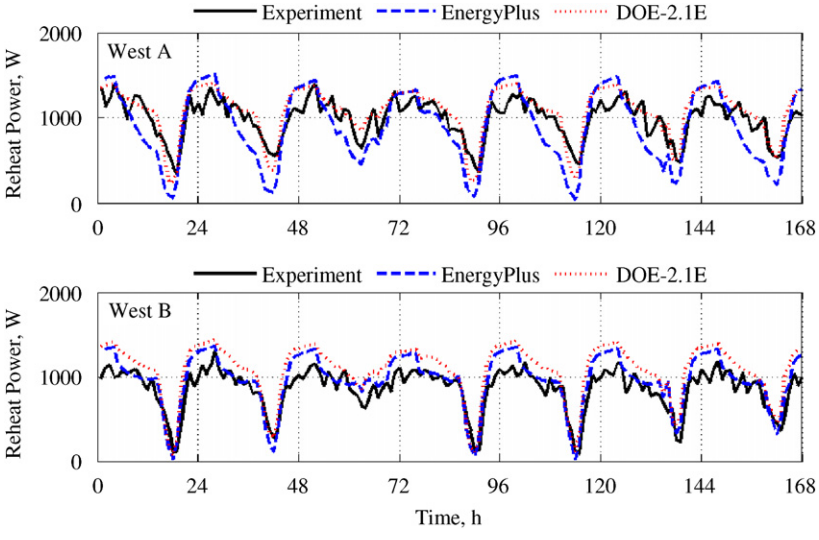

Fig. 16. Reheat coil power for the west test rooms.

Table 9
Statistical analysis for the room reheat coil power

	Units	East A		East B		South A			South B		West A			West B		
		Exp.	EnergyPlus	Exp.	EnergyPlus	Exp.	EnergyPlus	DOE-2.1E	Exp.	EnergyPlus	Exp.	EnergyPlus	DOE-2.1E	Exp.	EnergyPlus	DOE-2.1E
$\bar{x}$	W	809.1	948.7	864.7	843.1	1028.8	935.6	998.8	828.0	914.2	984.7	897.6	1075.5	876.6	983.7	1099.7
s	W	337.4	433.5	360.8	399.3	268.8	411.8	379.1	340.0	353.4	237.5	420.1	295.4	224.3	281.2	286.0
x_{max}	W	1284.0	1611.0	1378.0	1385.2	1433.0	1557.4	1439.4	1338.0	1425.6	1390.0	1511.4	1413.5	1308.0	1358.5	1428.8
x_{min}	W	3.0	0.0	2.0	0.0	410.0	96.0	133.7	31.0	138.4	339.0	37.8	231.7	87.0	142.9	158.7
$\overline{D}$	W	—	–139.7	—	21.7	—	93.3	30.0	—	–86.3	—	87.1	–90.9	—	–107.1	–223.0
$\lvert\overline{D}\rvert$	W	—	229.0	—	111.6	—	172.2	133.8	—	115.3	—	232.6	137.5	—	142.9	236.1
D_{max}	W	—	494.8	—	356.5	—	524.5	524.4	—	295.6	—	555.8	414.6	—	376.5	510.5
D_{min}	W	—	3.0	—	0.0	—	7.3	0.5	—	0.6	—	0.1	0.5	—	1.7	3.2
D_{rms}	W	—	262.0	—	136.8	—	205.3	178.8	—	136.6	—	272.9	165.6	—	175.4	261.1
$D_{95\%}$	W	—	419.5	—	253.7	—	413.6	377.5	—	234.5	—	487.1	297.9	—	329.6	419.3
$\overline{OU}$	W	1.8	90.3	2.0	87.5	2.3	87.9	–	1.9	87.6	2.2	91.3	—	2.0	88.4	—
$\overline{UR}$	—	—	2.5	—	1.2	—	1.9	1.5	—	1.3	—	2.5	1.5	—	2.7	3.7
UR_{max}	—	—	13.1	—	3.9	—	5.9	5.9	—	3.3	—	6.8	4.6	—	98.9	89.7
UR_{min}	—	—	0.0	—	0.0	—	0.1	0.0	—	0.0	—	0.0	0.0	—	0.0	0.0
$\lvert\overline{D}\rvert/\bar{x} \times 100\%$	%	—	28.3	—	12.9	—	16.7	13.0	—	13.9	—	23.6	14.0	—	16.3	26.9
$\overline{D}/\bar{x} \times 100\%$	%	—	–17.3	—	2.5	—	9.1	2.9	—	–10.4	—	8.8	–9.2	—	–12.2	–25.4
N	—	158	158	160	160	168	168	168	168	168	168	168	168	163	163	163

statistical analyses were only performed when the sum of the credible limits was greater than 1.0 W—done to ensure conceivable calculations for the uncertainty ratios. This criterion limited the extent of the analysis and excluded results when the lights were turned off by the controllers and the programs because credible limits were equal to zero during this time. Despite this limitation, the statistics do provide a good basis for comparisons and program assessment.

The light powers in the rooms were directly correlated to the illuminance predictions at low daylight levels. When the daylight illuminances at the reference points exceeded the set points in the rooms (700 Lux for the south test rooms and 645 Lux for the east and west test rooms), the lights were turned off; therefore, discrepancies in predictions for daylight illuminance reference points at higher values than the set point did not result in inconsistencies in the light power predictions.

For the east test rooms, accurate daylight illuminance predictions at the reference points when diffuse radiation entered the space translated into accurate light power predictions from EnergyPlus in the East B room (motorized mini-blinds). In the East A test room, the results mimicked the general trend of the experiment, but were not entirely consistent with the experiment.

In the South A test room, the over-predictions from both programs resulted in too much dimming in the space. In the South B test room, the EnergyPlus blind model (in the absence of beam radiation entering the space) performed quite well correlating illuminance predictions to light power. Again this accuracy is under-stated in the statistical analysis because of the cutoff criterion employed for evaluating statistical parameters.

In the west test rooms, the exterior shading algorithms in the programs accounted for the absence of beam radiation incident on the window until the afternoon when the sun was setting. For both test rooms, EnergyPlus and DOE-2.1E generally under-predicted the light power (over-predicted the daylight illuminance at the reference point). Difference in program predictions in the West A test room where shading screens were used can be attributed to differences in the program shading models. In the West B test room, the same exterior shading model was used with the same window models and differences can be accounted for by comparing the daylight model differences (EnergyPlus used four sky models compared with two used in DOE-2.1E) and room geometries (the DOE-2.1E model assumes the test rooms are cuboids).

7.3. Reheat coil power

The statistical comparisons for the reheat coil power reveal that none of the predictions were within 95% credible limits. The credible limits from the MCA were much larger than from the experiment. This is due to the high uncertainties associated with thermophysical properties, optical properties (particularly solar transmittance and

reflectance), thermal transmittances of the window, room set points (airflow rates and temperatures), which all impacted the load calculations and the required reheat coil power predictions. The experimental uncertainties only reflect the uncertainties associated with measurement of the electrical power to the coils, but do not factor in the uncertainties of the entering and leaving coil air temperatures and airflow rates, which most certainly added additional levels of uncertainty to the measurement beyond the scope of this study.

Generally, the results from EnergyPlus and DOE-2.1E are quite close; during the day differences between the programs can be attributed to the modeling of the interior shading screens that were also apparent for daylight illuminance predictions. Less robust inputs were also used in DOE-2.1E to describe the heat transfer between the shading screen air gap and interior window pane, but there seems to be little difference between the reheat coil predictions for the east test rooms where shading screens were installed in the East A test room and interior shading was not used in the East B test room; therefore the shade air gap modeling assumption does not appear to significantly impact the results. EnergyPlus also contains more robust algorithms for accounting for the interior convective and radiative heat transfer in the space and a more detailed heat transfer model for making transient load predictions; these resulted in slightly better zone thermal load predictions and, therefore, better reheat coil power predictions.

8. Conclusions

While the daylight algorithms and associated interactions for EnergyPlus and DOE-2.1E performed quite well, none of the parameters were validated within 95% credible limits. In general, the blind model implemented in EnergyPlus accurately predicted visible transmittance with the window/mini-blind assembly and the controllers accurately equated daylight illuminance predictions to light power adjustments (dimming or brightening the light). However, the limitations of the model were clearly seen when beam radiation entered the space. The program also seems quite flexible when making predictions for different types of windows and combinations of shades for different façade orientations.

From these results, both programs provided good estimates for building load calculations and reheat coil power. However, DOE-2.1E does not contain a model for mini-blinds, which severely limits the application of the program because mini-blinds are commonly installed in office spaces.

This study does provide confidence that both daylighting algorithm implementation do predict with some accuracy daylight illuminance and the associated interactions. These programs can provide insight into potential energy savings associated with the implementation of daylight controls in an office space. Building energy simulation programs can also be very valuable tools in the design phase of a new building to assess potentially daylight control savings by performing parametric studies varying windows and shading devices to optimize the energy performance of a building.

An indicator of overall performance during the experiment is the average differences between measured and predicted parameters. For EnergyPlus, the reference point daylight illuminance, light power, and reheat coil power predictions were within 119.2%, 16.9%, and 17.3%, respectively. DOE-2.1E predicted reference point daylight illuminances were within 114.1%, light powers were within 26.3%, and reheat coil power were within 25.4%. These values were averaged using the data of all test setups. However, much better results were realized for both programs in specific test rooms for all comparison parameters.

This paper provides assessments of the capacity of building energy simulation programs when simulating daylighting in a real building. The advantage of this type of validation is that nearly all the inputs about the constructing of the room, particularly the optical properties and fixture illuminances and powers that impacted the daylighting calculations, are known and well-described inputs to the programs. This allowed for accurate comparisons, within levels of experimental uncertainties, of the programs and a foundation for adjusting algorithms contained in building energy simulation programs to reflect actual building performance. Additionally, this study has also revealed the complexity associated with making daylighting predictions in building energy simulation program. In general, this exercise reveals how important robust empirical validations are for identifying deficiencies in building energy simulation programs. These building energy simulation tools provide practical computationally efficiently solutions for assessing the annual energy performance of daylighting applications and the associated interactions in buildings. However, better results can be obtained by using daylight autonomies in conjunction with the software, but the amount of time to construct and a run these types models makes them expensive for initial building design applications of actual buildings.

Acknowledgements

We would like to gratefully acknowledge the financial support of the Iowa Energy Center under Grant 9608. We would also like to thank the people at the Wisconsin Energy Center for providing the windows and the people at Nysan Shading Systems Inc. for the shading screens. We would like to acknowledge Som Shrestha for his hard work in designing and implementing the motorized blind controls. We would also like to recognize the staff at the Energy Resource Station for their assistance in running these experiments. The people specifically involved in this endeavor included: Curt Klaassen, Dave Perry, Xiao Hui

Zhou, and Emir Kadic. We also thank the staff at EMPA for performing optical measurements; these people included: Martin Camenzind and Kaethe Meyer.

References

[1] Judkoff RD. Validation of building energy analysis simulation programs at the solar energy research institute. Energy Build 1988;10:221–39.
[2] Gugliermetti F, Bisegna F. Daylighting with external shading devices: design and simulation algorithm. Build Environ 2006;14:136–49.
[3] Park K, Athienitis AK. Workplace illuminance prediction method for daylighting control systems. Solar Energy 2003;75:277–84.
[4] Tzempelikos A, Athienitis AK. Integrated thermal and daylighting analysis for design of office buildings. ASHRAE Trans 2005;111(1): 227–38.
[5] Park K, Athienitis AK. Development and testing of an integrated daylighting control system. ASHRAE Trans 2005;111(1):218–26.
[6] Bellia L, Cesarano A, Minisheillo F, Sibilio S. De-Light: a software tool for the evaluation of direct daylighting illuminances both indoors and outdoors-comparison with Superlite 2.0 and Lumin Micro 7.1. Build Environ 2000;35:281–95.
[7] Johnsen K. Daylight in buildings, Collaborative research in the International Energy Agency (IEA Task 21). Renewable Energy 1998;15:142–50.
[8] Winkelmann FC, Selkowitz S. Daylighting simulation in DOE-2 building energy analysis program. Energy Build 1985;8(5):271–86.
[9] Loutzenhiser PG, Maxwell GM. A comparison of DOE-2.1E daylighting and HVAC system interactions to actual building performance. ASHRAE Trans 2006;112(2).
[10] Loutzenhiser PG. Empirical validations of the DOE-2.1E building simulation software for daylighting and economizer controls. Thesis (Masters), Iowa State University, Ames, Iowa; 2003.
[11] Maxwell GM, Loutzenhiser PG, Klaassen C. Daylighting—HVAC interaction tests for the empirical validation of building energy analysis tools. A Report of IEA Task 22, Subtask D Building Energy Analysis Tools Project D Empirical Validation, 〈http://www.iea-shc.org/task22〉 2003.
[12] Lee S. Empirical validation of building energy simulation software: DOE-2.1E, HAP, and TRACE. Thesis (PhD), Iowa State University, Ames, Iowa; 1999.
[13] Kuiken TA, Energy savings in a commercial building with daylighting controls : empirical study and DOE-2 validation. Thesis (Masters), Iowa State University, Ames, Iowa; 2002.
[14] Bodart M, De Herde A. Global energy savings in offices buildings by use of daylighting. Energy Build 2002;34:421–9.
[15] Li DHW, Lam JC, Wong SL. Daylighting and its effect on peak load determination. Energy 2005;30:1817–31.
[16] Gates S, Wilcox J. Daylighting analysis for classrooms using DOE-2.1b. Energy Build 1984;6:4:331–41.
[17] Hart GH, Blancett RS, Charter KF. The use of DOE-2 to determine the relative energy performance of daylighted retail stores covered with tension supported fabric roofs. Energy Build 1984;6(4):343–52.
[18] Strachan P. Model Validation using the PASSYS test cells. Build Environ 1993;28:153–65.
[19] Wouters P, Vandaele L, Voit P, Fisch N. The use of outdoor test cells for thermal and solar building research within the PASSYS project. Build Environ 1993;28:107–13.
[20] Jensen SØ. Validation of building energy simulation programs: a methodology. Energy Build 1995;22:133–44.
[21] Lomas KJ, Eppel H, Martin CJ, Bloomfield DP. Empirical validation of building energy simulation programs. Energy Build 1997;26: 253–75.
[22] Manz H, Loutzenhiser P, Frank T, Strachan PA, Bundi R, Maxwell G. Series of experiments for empirical validation of solar gain modeling in building energy simulation codes—experimental setup, test cell characterization, specifications and uncertainty analysis. Build Environ 2004;41:1784–97.
[23] Loutzenhiser PG, Manz H, Felsmann C, Strachan PA, Frank T, Maxwell GM. Empirical validation of models to compute solar irradiance on inclined surfaces for building energy simulation. Solar Energy 2007;81:254–67.
[24] Loutzenhiser PG, Manz H, Strachan PA, Felsmann C, Frank T, Maxwell GM, Oelhafen P. An empirical validation of solar gain models found in building energy simulation programs. HVAC&R Res 2006;12(4):1097–116.
[25] Loutzenhiser PG, Manz H, Felsmann C, Strachan PA, Maxwell GM. An empirical validation of modeling solar gain through a glazing unit with external and internal shading screens. Appl Thermal Eng 2007;27:528–38.
[26] EnergyPlus Software (Version 1.4.0.025), Building Energy Simulation Code, 〈http://www.energyplus.gov〉 2006.
[27] DOE-2.1E (Version-119) Building Energy Simulation Code, Lawrence Berkley Laboratories (LBL), Berkley, CA, April 9, 2002.
[28] Price BA, Smith TF. Description of the Iowa Energy Center Energy Resource Station: Facility Update III, University of Iowa, Iowa City, IA, 2000.
[29] European Standard EN 410. Glass in building—Determination of luminous and solar characteristics of glazing. European Committee for Standardization, Brussels, Belgium, 1998.
[30] GLAD Software. Swiss Federal Laboratories for Materials Testing and Research (EMPA). Duebendorf, Switzerland, 2002.
[31] Winkelmann FC, Birdsall BE, Buhl WF, Ellington KL, Erdem AE, Hirsch JJ, et al. DOE-2 Supplement Version 2.1E. LBL-34947, November 1993
[32] EnergyPlus. Engineering Reference, Board of Trustees of University of Illinois and the University of California through Orlando Lawrence Berkley Laboratories. October 11, 2005.
[33] Perez R, Ineichen P, Seals R, Michalsky J, Stewart R. Modeling daylight availability and irradiance components from direct and global irradiance. Solar Energy 1990;44:271–89.
[34] Ineichen P, Perez R, Seals R. The importance of correct albedo determination for adequately modeling energy received by a tilted surface. Solar Energy 1987;39(4):301–5.
[35] Window 5.2a. Version 5.2.17a, LBL, August 1, 2005.
[36] ISO/FDIS 15099: 2003(E), Thermal performances of windows, doors, and shading devices—Detailed calculations, 2003.
[37] Walton GN. Thermal analysis research program reference manual. NBSIR 83-2655, March 1983; p. 21.
[38] Clark G, Allen C. The estimation of atmospheric radiation for clear and cloudy skies. In: Proceedings of the second national passive solar conference (AS/ISES); 1978. p. 675–8.
[39] EN ISO 6946. Building components and building elements—Thermal resistance and thermal transmittance—Calculation Method, August 1996.
[40] Gleser GL. Assessing Uncertainty in Measurement. Statistical Science 1998;13:3:277–90.